New On-sky results from FASS

A. Guesalaga[1*], B. Ayancán[1], H. González[1], S. Perera[3], M. Sarazin[2], J. Navarrete[2], J. Osborn[3], T. Butterley[3], R. Wilson[3], B. Neichel[4], K. El Hadi[4]

[1]P. Universidad Católica, Chile; [2]European Southern Observatory, Germany; [3]Durham University, United Kingdom; [4]LAM, Marseille, France

ABSTRACT

FASS (Full Aperture Scintillation Sensor [1]) provides estimates of $C_n^2(h)$ profiles, together with seeing, coherence time, Fried parameter and isoplanatic angle. The monitor is meant for site testing and to support operations of very large telescopes and future ELTs. The key components of the instrument are a low-noise camera (sCMOS or CCD) attached to a portable telescope (9.5” or 12”) that together with a customized optics, processes scintillation images. These “flying shadows” or speckles are subsequently processed to get their power spectra that, fitted to a linear combination of previously simulated scintillation images from single turbulence layers located at different altitudes, yield estimates of stratified turbulence strengths.

We present new results using on-sky data provided by a basic optical set-up, configured for the free-atmosphere case ($z > 500\ m$). The results are compared to profiles simultaneously acquired from a stereo-SCIDAR instrument installed in one of Paranal AT telescopes [2] and from MASS/DIMM estimates. Despite a non-optimal optical configuration, encouraging results have been obtained during 2018 campaigns at Paranal observatory.

1. THE FASS CONCEPT: THE PUPIL CONJUGATION CASE

In the FASS technique, the incoming light captured by a small size telescope (9.5” or 12”) is transferred to the detector, generating an image of the pupil containing scintillation patterns (speckles). The full aperture of the telescope is sampled (hence the name FASS, Full Aperture Scintillation Sensor). In the pupil conjugation mode, the telescope pupil is imaged. In this configuration, near-the-ground turbulence are invisible due to the lack of scintillation contrast and speckle sizes that are similar to those of the detector the pixels, making the estimation of the ground layer impossible.

A clear difference exists in scintillation patterns from turbulence layers at different heights; smaller speckles correspond to layers near the ground (left image); larger ones are from upper layers (right image).

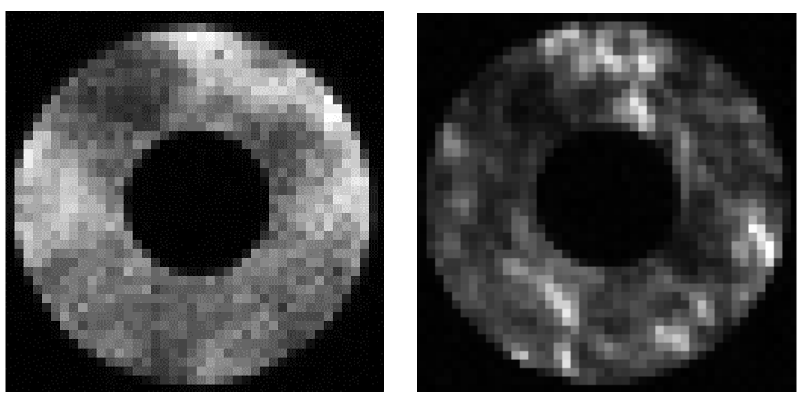

Figure 1- Scintillation patterns. Left: low altitude turbulence; right: high altitude turbulence (Celestron 9.5” telescope, April 2018, Paranal)

This phenomena can be explained by the Fresnel formula $d_s \approx \sqrt{z\lambda}$, where d_s is the speckle size, z is the distance to the layer and λ is the light wavelength, of a monochromatic source.

*aguesala@ing.puc.cl

Fresnel law: speckle size

$$d_s \approx \sqrt{z\lambda}$$

For λ = 500 nm:

d_s @ 0.5km = 1.6 cm

d_s @ 20km = 10.0 cm

Pupil images at the detector are transformed to a polar grid formed by concentric rings. The polar grid is unraveled to one or more concentric rings. In the image, five rings are unraveled, Fourier-transformed and averaged.

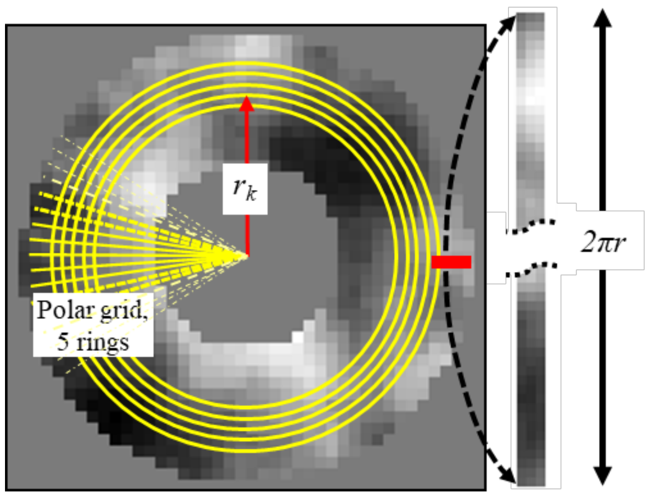

Figure 2- Unravelling the rings

The benefits of unravelling the annulus is three-fold:

- It reduces the impact of diffraction rings from inner and outer pupil edges. This is of great relevance for the generalized version to be described later.
- Larger speckles (from higher altitude layer) can be processed, due to sampling along the $2\pi r$ rings (r is the central radius of the resampled rings)
- The Fourier-transform is performed for a circular, continuous 1-D vector, avoiding contamination of the spectra due to ringing caused by discontinuities

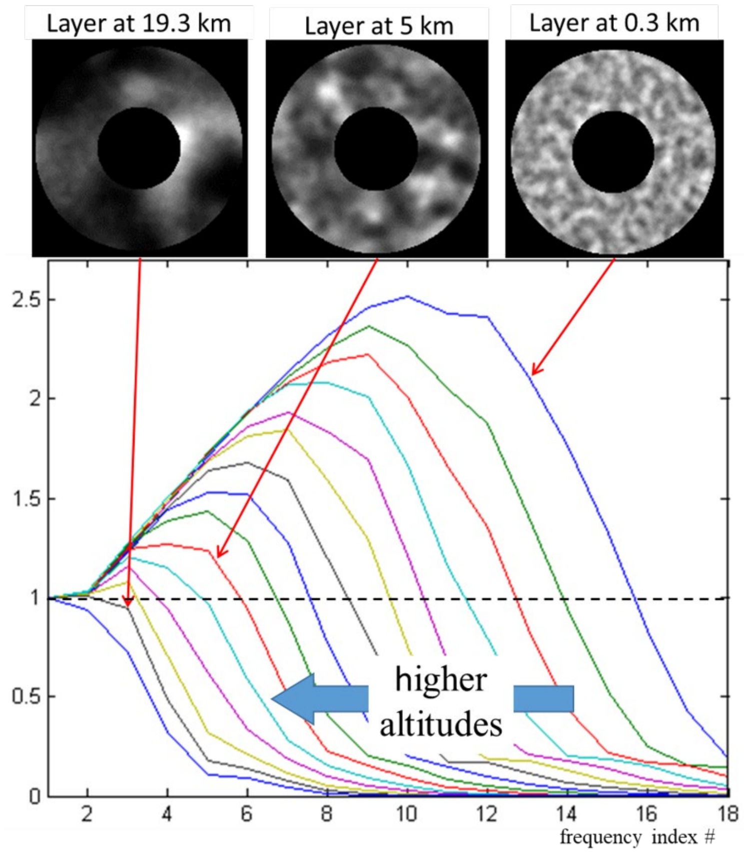

Figure 3- Normalized weighting functions obtained from unravelled rings

By calculating the average power spectra for each unravelled array and repeating this procedure for a large number of images, we get its average spectrum. This process is performed for real pupil images and for reference spectra from simulated images. The reference spectra correspond to single layers located at increasing heights; they form the basis for the inversion problem of estimating the turbulence profile out of pupil images.

A family of 15 spectra (herein weighting functions) are constructed from 12,000 images for layers located at the following heights: $Z = \{0.3, 0.45, 0.6, 0.8, 1.05, 1.4, 1.9, 2.6, 3.6, 5.0, 6.9, 9.6, 13.8, 19.3, 27.3\}$ km

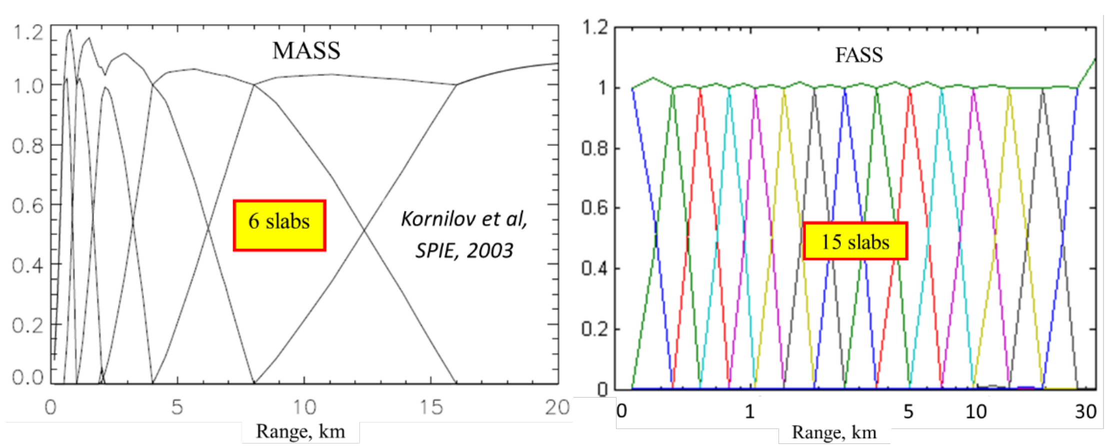

Figure 4- Theoretical response functions: MASS (left); FASS (right)

One way to evaluate the nominal accuracy of the technique is by comparing its response to a layer scanning the full range of distances. Figure 3 shows the performances of MASS [3] and FASS. The first advantage of the latter is its larger number of slabs that form the profile (6 to 15). The accuracy measured by the sum of slabs combinations for altitudes different from those of the reference set are substantially better that for MASS (the departure from unity is much smaller in the case of FASS).

Another appealing feature of FASS is that the number of slabs and the weighting functions used, can be adapted to observation conditions i.e. air mass, seeing and star spectrum and brightness.

2. APRIL 2018 CAMPAIGN, PARANAL

We tested the technique against a stereo-SCIDAR [2], a high-resolution monitor that also uses scintillation as the principle of probing the atmosphere. During this campaign held at Paranal, (Chile) SCIDAR was installed in one of the 1.8m AT telescopes with its optics negatively conjugated. This was not the case for FASS that run with the standard configuration (free-atmosphere), which is blind to ground turbulence.

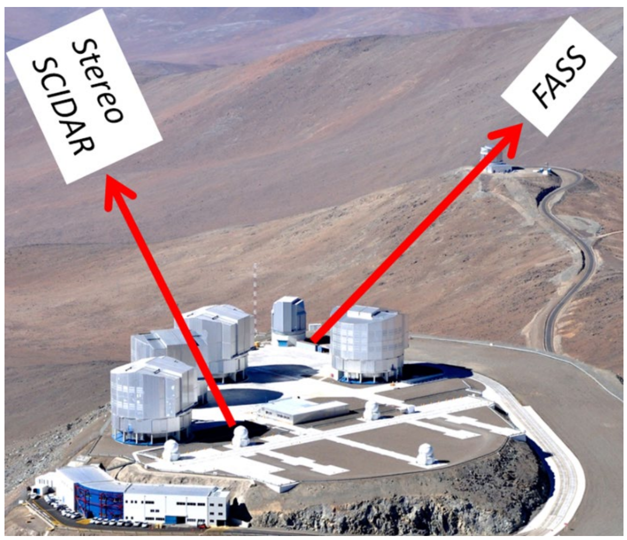

Figure 4- FASS and Stereo SCIDAR at Paranal: Each instrument probes a different portion of the atmosphere

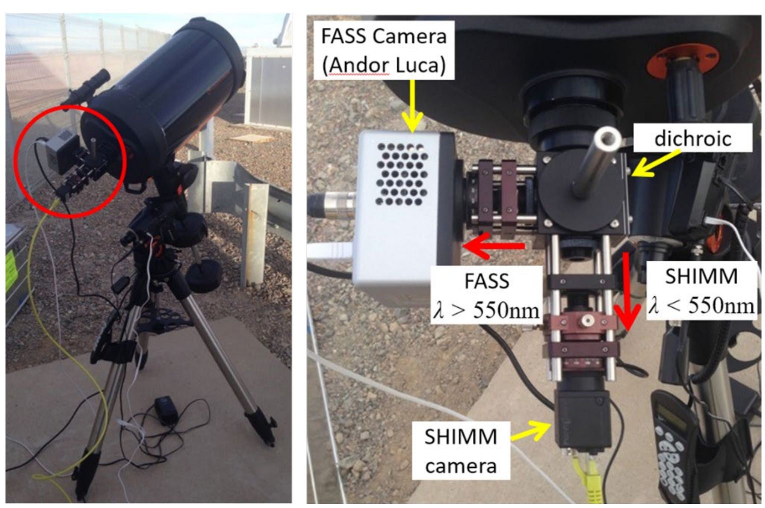

Figure 5- FASS optical set-up: The light collected from the a 9.5" telescope is shared by the SHIMM monitor [5] and FASS

Figure 6 shows an example of the estimated profiles for FASS (top) and SCIDAR (bottom) during the April, 2018 campaign. The Stereo-SCIDAR resolution has been reduced to match that of FASS. A remarkable resemblance between both instruments is observed, despite looking through different air masses and directions. The estimations are for the free-atmosphere case (h>1Km) as the FASS monitor is in the standard mode (pupil conjugation)

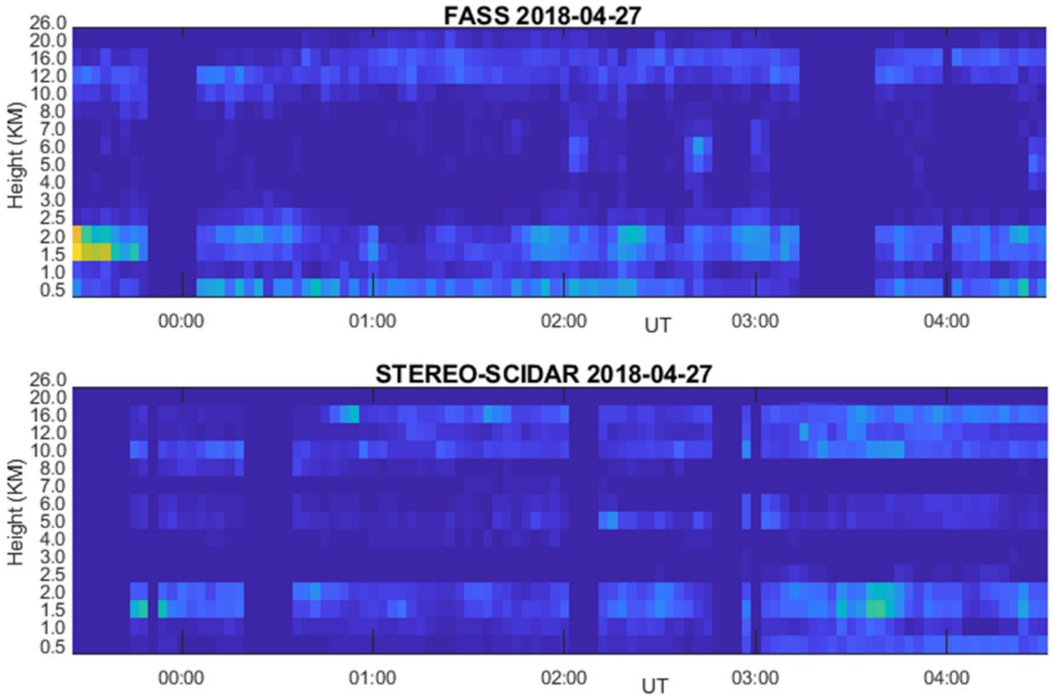

Figure 6. Example of simultaneous profiles: FASS vs Stereo SCIDAR

Figure 7 shows a correlation plot for seeing values for FASS and MASS monitors for the entire campaign (time-stamp difference less than 3 minutes). An excellent matching is seen.

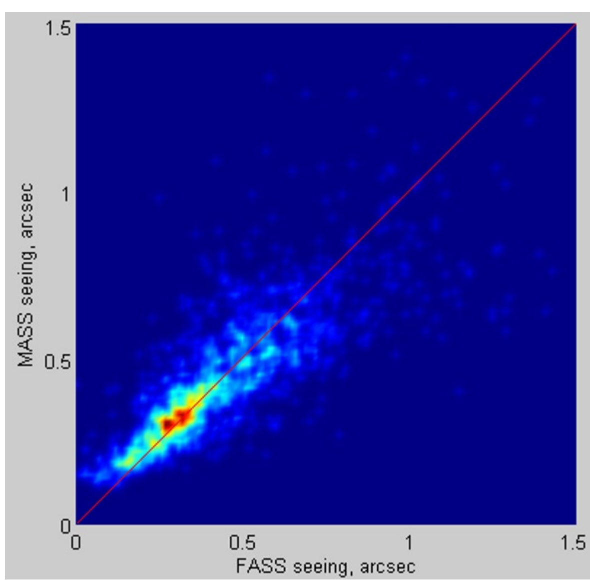

Figure 7- Total seeing correlation between FASS and MASS monitors during 2018 campaigns at Paranal

3. THE GENERALIZED FASS: THE NEGATIVE CONJUGATION CASE

We aim to develop a generalized version of FASS that includes the ground layer, so making DIMM redundant. The weakness of monitors based on scintillation is their blindness to measure turbulence strength located near the ground. The obvious solution to overcome this problem is to allow the propagation of the distorted wavefront below the telescope pupil by means of additional optics [4]. The problem with such approach is the diffraction caused by the telescope aperture masking on the subsequent negatively conjugated images.

Simulations show that this undesired effect occurs even at short negative conjugations. The simulated image is formed at a conjugation of -300 m below the pupil. Diffraction rings are clearly visible, making the frequency analysis described above extremely difficult. The scintillation image is sampled circularly and continuously, so this effect is substantially mitigated. This problem is not entirely eliminated, so an apodizer is introduced.

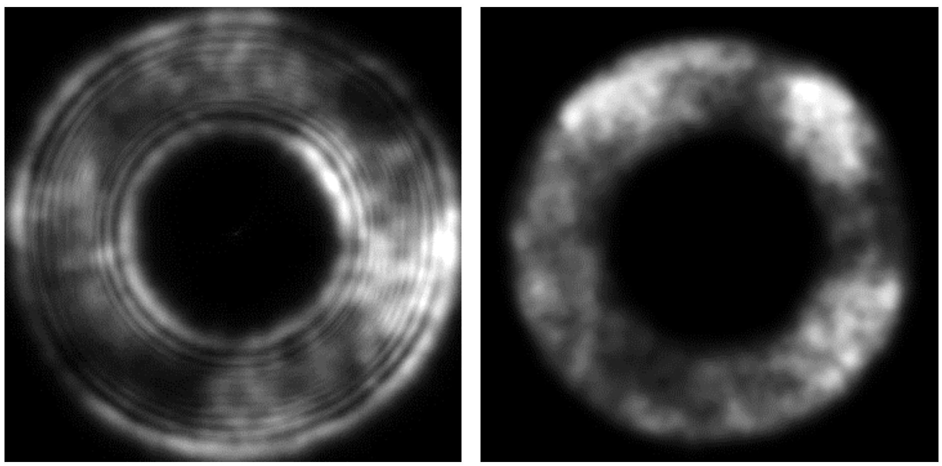

Figure 8- Result of applying an apodization mask to a scintillation image formed 300 m below the pupil. The strong diffraction rings observed with no apodization (left) disappear when the mask is applied (right), at the cost of a narrower aperture annulus.

Figure 9 shows the optical schematics for the generalized FASS. At the detector plane negatively conjugated at -300 m, an image of the pupil is formed. A 4f system comprising two identical lenses (L_1 and L_2) allows to include the apodizer and a 100 nm width spectral filter to limit the wavelengths to be used.

The detector plane is negatively conjugated at -300m. A 4f system comprising two identical lenses (L_1 and L_2) allows to include an apodizer and a 100 nm width spectral filter to limit the wavelengths to be used.

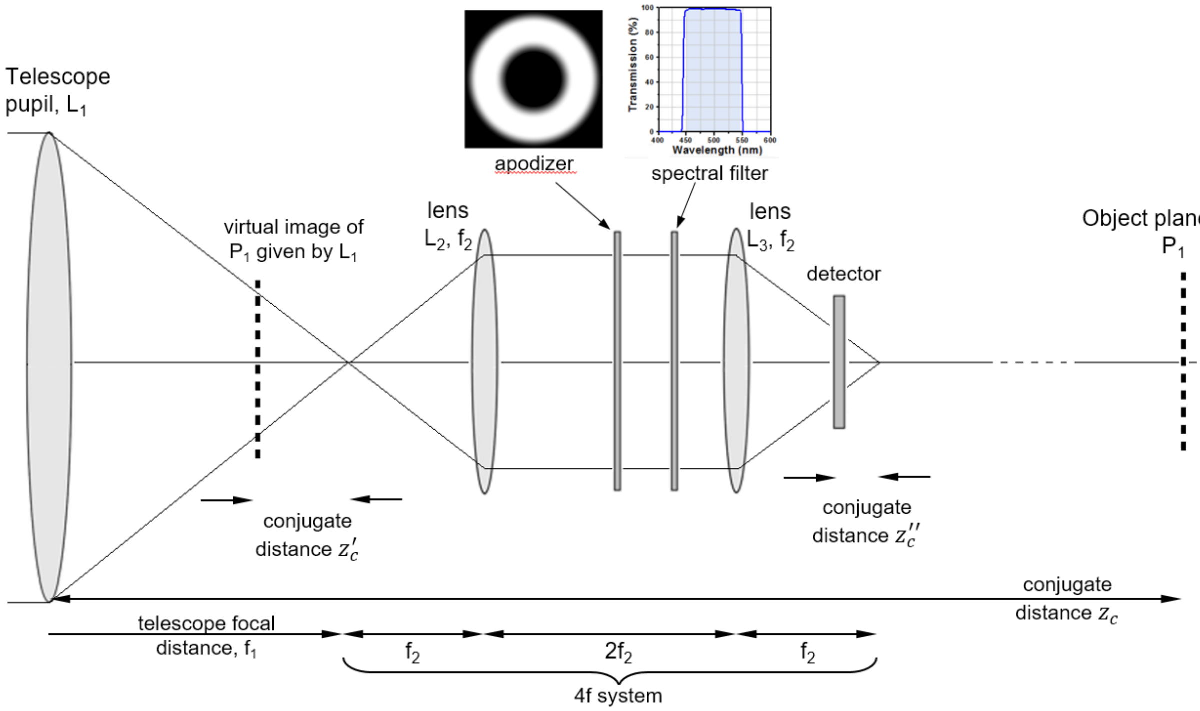

Figure 9- Generalized FASS, optical set-up

4. CONCLUSIONS

The FASS concept has been validated on-sky by comparing its performance against the Stereo-SCIDAR system and MASS-DIMM monitor for the free-atmosphere case. Although the pointing of the three monitors differed during the tests, good correlation among the profile were obtained.

The next step is to develop a generalized version of FASS, where a conjugation of -300 m has shown to be an excellent choice to balance the associate diffraction with the minimum contrast and speckle size required for a good performance of the method.

ACKNOWLEDGEMENTS
This project is supported by the Chilean National Science Foundation (CONICYT), project Fondecyt 1190186.

[1] Guesalaga A., Perera S., Osborn J., et al, 2016, Proc. SPIE 9909, 99090H
[2] Osborn J., Wilson R.W., Sarazin M., et al, MNRAS, 825, 2018
[3] Kornilov V.,Tokovinin A.,Voziakova O., et al, 2003, Proc. SPIE, 4839,837
[4] Kluckers V., Wooder N., Nicholls T., et al, A & A Sup.,130, p141, 1998
[5] Perera S., Wilson R.W., Osborn J., et al, 2016, Proc. SPIE 9909, 99093J